

Transfer Learning for Motor Imagery Based Brain-Computer Interfaces: A Complete Pipeline

Dongrui Wu^{a,b}, Xue Jiang^a, Ruimin Peng^a, Wanzeng Kong^b, Jian Huang^{a,*}, Zhigang Zeng^{a,*}

^aKey Laboratory of the Ministry of Education for Image Processing and Intelligent Control,
School of Artificial Intelligence and Automation,
Huazhong University of Science and Technology, Wuhan 430074, China
^bZhejiang Key Laboratory for Brain-Machine Collaborative Intelligence,
Hangzhou Dianzi University, Hangzhou 310018, China

Abstract

Transfer learning (TL) has been widely used in motor imagery (MI) based brain-computer interfaces (BCIs) to reduce the calibration effort for a new subject, and demonstrated promising performance. While a closed-loop MI-based BCI system, after electroencephalogram (EEG) signal acquisition and temporal filtering, includes spatial filtering, feature engineering, and classification blocks before sending out the control signal to an external device, previous approaches only considered TL in one or two such components. This paper proposes that TL could be considered in all three components (spatial filtering, feature engineering, and classification) of MI-based BCIs. Furthermore, it is also very important to specifically add a data alignment component before spatial filtering to make the data from different subjects more consistent, and hence to facilitate subsequential TL. Offline calibration experiments on two MI datasets verified our proposal. Especially, integrating data alignment and sophisticated TL approaches can significantly improve the classification performance, and hence greatly reduces the calibration effort.

Keywords: Brain-computer interface, EEG, transfer learning, Euclidean alignment, motor imagery

1. Introduction

A brain-computer interface (BCI) [16, 43] enables a user to communicate directly with an external device, e.g., a computer, using his/her brain signals, e.g., electroencephalogram (EEG). It can benefit both patients [31] and able-bodied people [41, 27].

*Corresponding authors

Email addresses: drwu@hust.edu.cn (Dongrui Wu), xuejiang@hust.edu.cn (Xue Jiang), rmpeng2019@hust.edu.cn (Ruimin Peng), kongwanzeng@hdu.edu.cn (Wanzeng Kong), huang_jan@hust.edu.cn (Jian Huang), zgzung@hust.edu.cn (Zhigang Zeng)

Motor imagery (MI) [32] is a common paradigm in EEG-based BCIs, and also the focus of this paper. In MI-based BCIs, the user imagines the movements of his/her body parts, which activates different areas of the motor cortex of the brain, e.g., top-left for right-hand MI, top-right for left-hand MI, and top-central for feet MI. A classification algorithm can then be used to decode the recorded EEG signals and map the corresponding MI to a command for the external device.

The flowchart of a closed-loop EEG-based BCI system is shown in Figure 1. It consists of the following main components [50]:

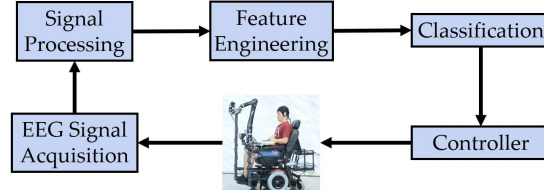


Figure 1: A closed-loop EEG-based BCI system, using MI as an example.

1. *Signal acquisition*, which uses a headset to collect EEG signal from the scalp, while the user is performing MI tasks.
2. *Signal processing* [22]. Because EEG signals are weak, and easily contaminated by artifacts and interferences, e.g., muscle movements, eye blinks, heartbeats, powerline noise, etc., sophisticated signal processing approaches must be used to increase the signal-to-noise ratio. Both temporal filtering and spatial filtering are usually performed. Temporal filtering may include notch filtering to remove the 50Hz or 60Hz powerline interference, and then bandpass filtering, e.g., [8, 30] Hz, to remove DC drift and high frequency noise. Spatial filters [45] include the basic ones, e.g., common average reference [40], Laplacian filters [15], principal component analysis [12], etc., and more sophisticated ones, e.g., independent component analysis [7], xDAWN [35], canonical correlation analysis [37], common spatial patterns (CSP) [33], etc.
3. *Feature engineering*, which includes feature extraction, and sometimes also feature selection. Time domain, frequency domain, time-frequency domain, Riemannian space [52], and/or topoplot features [18] could be used.
4. *Classification* [23], which uses a machine learning algorithm to decode the EEG signal from the extracted features. Commonly used classifiers include linear discriminant analysis (LDA) and support vector machine (SVM).
5. *Controller*, which sends a command to an external device, e.g., a wheelchair, according to the decoded EEG signal.

Because of individual differences and non-stationarity of EEG signals, an MI-based BCI usually needs a long calibration session for a new subject, from 20-30 minutes [38] to hours or even days. This lengthy calibration significantly reduces the utility of BCI systems. Hence, many sophisticated signal processing and machine learning approaches have been proposed recently to reduce or eliminate the calibration [6, 9, 10, 11, 36, 42, 44, 50, 53, 54].

One of the most promising such approaches is transfer learning (TL) [28], which uses data/knowledge from source domains (existing subjects) to help the calibration in the target domain (new subject). However, previous TL approaches for BCIs usually considered only one or two components of the closed-loop system in Figure 1, particularly, classification, as introduced in our latest survey [50]. For example, Jayaram *et al.* [11] proposed a multi-task learning (which is a subfield of TL) framework for cross-subject MI classification. To consider TL in spatial filtering, Dai *et al.* [6] proposed transfer kernel CSP to integrate kernel CSP [1] and transfer kernel learning [21] for EEG trial filtering. To consider TL in feature engineering, Chen *et al.* [4] extended ReliefF [13] and minimum redundancy maximum relevancy (mRMR) [29] feature selection approaches to Class-Separate and Domain-Fused (CSDF)-ReliefF and CSDF-mRMR, which optimized both the class separability and the domain similarity simultaneously. They then further integrated CSDF-ReliefF and CSDF-mRMR with an adaptation regularization-based TL classifier [20].

In this paper, we claim that TL should be considered in as many components of a BCI system as possible, and propose a complete TL pipeline for MI-based BCIs, shown in Figure 2:

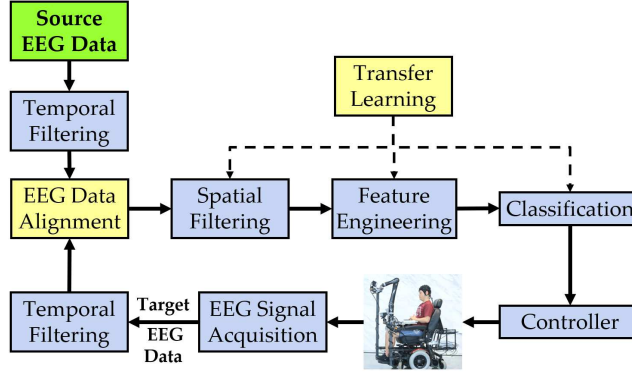


Figure 2: A complete TL pipeline for closed-loop MI-based BCI systems.

1. *Temporal filtering*, where band-pass filtering is performed on both the source and target domain data.
2. *Data alignment*, which aligns EEG trials from the source domains and the target domain so that their distributions are more consistent. This is a new component, which does not exist in Figure 1, but will greatly facilitate TL in sequential components, as shown later in this paper.
3. *Spatial filtering*, where TL can be used to design better spatial filters, especially when the amount of target domain labeled data is small.
4. *Feature engineering*, where TL may be used to extract or select more informative features.
5. *Classification*, where TL can be used to design better classifiers or regression models, especially when there are no or very few target domain labeled data.

We will introduce some representative TL approaches in data alignment, spatial filtering, feature selection and classification, and demonstrate using two MI datasets that incorporate TL in all these components can indeed achieve better classification performance than not using TL, or using TL in only a subset of these components.

Our main contributions are:

1. We propose a complete TL pipeline for closed-loop MI-based BCI systems, as shown in Figure 2, and point out that explicitly including a data alignment component before spatial filtering is very important to the TL performance, for both traditional machine learning and deep learning, both offline and online classification, and both cross-subject and cross-session classification.
2. We verify through experiments that usually considering TL in more components in Figure 2 can result in better classification performance, and more sophisticated TL approaches are usually more beneficial than simple TL approaches, or not using TL at all.

The remainder of this paper is organized as follows: Section 2 introduces some representative TL approaches at different components of a BCI system. Section 3 evaluates the performance of the complete TL pipeline in offline cross-subject MI classification. Section 4 discusses the TL pipeline in offline cross-subject classification using deep learning, online cross-subject classification, and offline cross-session classification. Finally, Section 5 draws conclusions and points out some future research directions.

2. TL Approaches

This section introduces the basic concepts of TL, and how TL could be used in data alignment, spatial filtering, feature selection and classification of an MI-based BCI system.

We consider offline binary classification only, and would like to use labeled EEG trials from a source subject to help classify trials from a target subject. When there are multiple source subjects, we can combine data from all source subjects and then view that as a single source subject, or perform TL for each source subject separately and then aggregate them.

Assume the source subject has N_s labeled samples $\{X_s^n, y_s^n\}_{n=1}^{N_s}$, where $X_s^n \in \mathbb{R}^{c \times t}$ is the n -th EEG trial and y_s^n the corresponding class label, in which c is the number of EEG channels, and t the number of time domain samples. The target subject has N_l labeled samples $\{X_t^n, y_t^n\}_{n=1}^{N_l}$, and N_u unlabeled samples $\{X_t^n\}_{n=N_l+1}^{N_l+N_u}$. In offline calibration, the N_u unlabeled samples are also known to us, and we need to design a classifier to obtain their labels.

2.1. TL

TL [28] uses data/knowledge from a source domain to help solve a task in a target domain. A domain consists of a feature space \mathcal{X} and its associated marginal probability distribution $P(X)$, i.e., $\{\mathcal{X}, P(X)\}$, where $X \in \mathcal{X}$. Two domains are different if they have different feature spaces, and/or different $P(X)$. A task consists of a label space \mathcal{Y}

and a prediction function $f(X)$, i.e., $\{\mathcal{Y}, f(X)\}$. Two tasks are different if they have different label spaces, and/or different conditional probability distributions $P(y|X)$.

For BCI calibration, TL usually means to use labeled EEG trials from an existing subject to help the calibration for a new subject. This paper considers the scenario that both subjects have the same feature space and label space, i.e., the subjects wear the same EEG headset and perform the same types of MIs, but different $P(X)$ and $P(y|X)$. This is the most commonly encountered TL scenario in BCI calibration.

A very simple idea of TL in classifier training is illustrated in Figure 3. Assume the target domain has only four training samples belonging to two classes (represented by different shapes), whereas the source domain has more. Without TL, we can build a classifier in the target domain using only its own four training samples. Since the number of training samples is very small, this classifier is usually unreliable. With TL, we can combine samples from the source domain with those in the target domain to train a classifier. Since the two domains may not be completely consistent, e.g., the marginal probability distributions may be different, we may assign the source domain samples smaller weights than the target domain samples. If optimized properly, the resulting classifier can usually achieve better generalization performance.

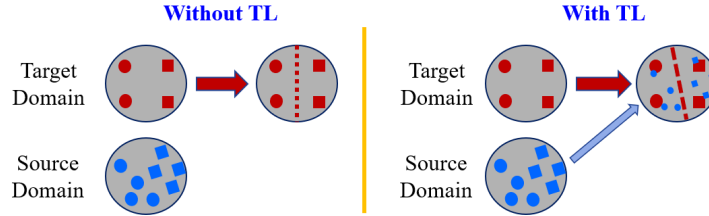


Figure 3: Illustration of simple TL in classification.

Figure 3 illustrates maybe the simplest TL approach in classification. Similar approaches may also be used in spatial filtering and feature engineering components in Figure 2. We will introduce some of them next.

2.2. Euclidean Alignment (EA)

Due to individual differences, the marginal probability distributions of the EEG trials from different subjects are usually (significantly) different; so, it is very beneficial to perform data alignment to make different domains more consistent, before other operations in Figure 2.

Different EEG trial alignment approaches have been proposed recently [9, 10, 36, 53, 54]. A summary and comparison of them is given in [50]. Among them, Euclidean alignment (EA), proposed by He and Wu [10] and illustrated in Figure 4, is easy to perform and completely unsupervised (does not need any labeled data from any subject). So, it is used as an example in this paper.

For the source subject, EA first computes

$$\bar{R}_s = \frac{1}{N_s} \sum_{n=1}^{N_s} X_s^n (X_s^n)^\top, \quad (1)$$

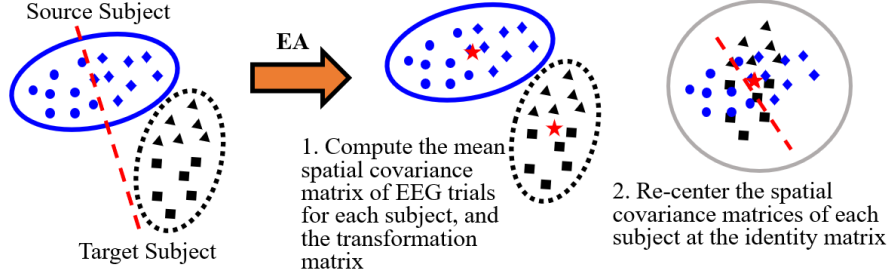


Figure 4: EA for aligning EEG trials from different subjects (domains).

i.e., the Euclidean arithmetic mean of all spatial covariance matrices from the source subject, then performs the alignment by

$$\tilde{X}_s^n = \bar{R}_s^{-1/2} X_s^n. \quad (2)$$

Similarly, for the target subject, EA computes the arithmetic mean of all $N_l + N_u$ spatial covariance matrices and then performs the alignment.

After EA, the aligned EEG trials are whitened [54], and their mean spatial covariance matrix from each subject equals the identity matrix [10]; hence, the distributions of EEG trials from different subjects become more consistent. This will greatly benefit TL in subsequent steps.

2.3. Pre-alignment Strategy (PS)

Xu et al. [51] proposed an online pre-alignment strategy (PS) to match the distributions from different domains. When used in offline classification, its formula is essentially identical to (2), except that the Riemannian mean [30] instead of the Euclidean mean is used in computing \bar{R}_s .

The *Riemannian distance* $\delta(R, R^n)$ between two symmetric positive-definite covariance matrices $R \in \mathbb{R}^{c \times c}$ and $R^n \in \mathbb{R}^{c \times c}$ is the minimum length of a curve connecting them on the Riemannian manifold, computed as [26]:

$$\delta(R, R^n) = \|\log(R^{-1}R^n)\|_F = \left[\sum_{i=1}^c \log^2 \lambda_i \right]^{\frac{1}{2}}, \quad (3)$$

where the subscript $_F$ denotes the Frobenius norm, and λ_i , $i = 1, \dots, c$, are the real eigenvalues of $R^{-1}R^n$.

The *Riemannian mean* [30] of N covariance matrices is defined as the matrix minimizing the sum of the squared Riemannian distances, i.e.,

$$\bar{R} = \arg \min_R \sum_{n=1}^N \delta^2(R, R^n). \quad (4)$$

The Riemannian mean does not have a closed-form solution, but can be computed by an iterative gradient descent algorithm [8].

The characteristics of PS are almost identical to EA, i.e., it is completely unsupervised, and aligns the EEG trials directly, except that its computational cost is higher than EA, as the Riemannian mean does not have a closed-form solution.

2.4. CSP

CSP [3, 33] performs supervised spatial filtering for EEG trials, aiming to find a set of spatial filters to maximize the ratio of variance between two classes.

The traditional CSP uses data from the target subject only. For Class $k \in \{-1, 1\}$, CSP tries to find a spatial filter matrix $W_k^* \in \mathbb{R}^{c \times f}$, where f is the number of spatial filters, to maximize the variance ratio between Class k and Class $-k$:

$$W_k^* = \arg \max_{W \in \mathbb{R}^{c \times f}} \frac{\text{tr}(W^\top \bar{C}_t^k W)}{\text{tr}(W^\top \bar{C}_t^{-k} W)}, \quad (5)$$

where $\bar{C}_t^k \in \mathbb{R}^{c \times c}$ is the mean spatial covariance matrix of the N_l labeled EEG trials in Class k , and tr the trace of a matrix. The solution W_k^* is the concatenation of the f leading eigenvectors of $(\bar{C}_t^{-k})^{-1} \bar{C}_t^k$.

Then, CSP concatenates the $2f$ spatial filters from both classes to obtain the complete filter matrix:

$$W^* = [W_{-1}^* \quad W_1^*] \in \mathbb{R}^{c \times 2f}, \quad (6)$$

and computes the spatially filtered X_t^n by:

$$\tilde{X}_t^n = W^{*\top} X_t^n \in \mathbb{R}^{2f \times t}. \quad (7)$$

Finally, the log-variances of \tilde{X}_t^n can be extracted as features $\mathbf{x}_t^n \in \mathbb{R}^{1 \times 2f}$ in later classification:

$$\mathbf{x}_t^n = \log \left(\frac{\text{diag} \left(\tilde{X}_t^n \left(\tilde{X}_t^n \right)^\top \right)}{\text{tr} \left(\tilde{X}_t^n \left(\tilde{X}_t^n \right)^\top \right)} \right), \quad (8)$$

where diag means the diagonal elements of a matrix, and \log is the logarithm operator.

2.5. Combined CSP (CCSP)

Because the target subject has very few labeled samples, i.e., N_l is small, W^* computed above may not be reliable. The source domain samples can be used to improve W^* .

In the combined CSP (CCSP), we simply concatenate the N_s source domain labeled samples and N_l target domain labeled samples to compute W^* . Note that all samples have the same weight, i.e., source domain and target domain samples are treated equally.

CCSP may be the simplest TL-based CSP approach.

2.6. Regularized CSP (RCSP)

Regularized CSP (RCSP) [24] was specifically proposed to handle the problem that the target domain has very few labeled samples. Though the original paper did not mention TL, it actually used the idea of TL.

RCSP computes the regularized average spatial covariance matrix for Class k as:

$$\hat{C}^k(\beta, \gamma) = (1 - \gamma)\hat{C}^k(\beta) + \frac{\gamma}{c}\text{tr}(\hat{C}^k(\beta))I, \quad (9)$$

where β and γ are two parameters in $[0, 1]$, $I \in \mathbb{R}^{c \times c}$ is an identity matrix, and

$$\hat{C}^k(\beta) = \frac{\beta N_l \bar{C}_t^k + (1 - \beta) N_s \bar{C}_s^k}{\beta N_l + (1 - \beta) N_s}. \quad (10)$$

$\hat{C}^k(\beta, \gamma)$ can then be used to replace \bar{C}_t^k in (5) to compute the CSP filter matrix.

Note that when $\beta = 1$ and $\gamma = 0$, RCSP becomes the traditional CSP. When $\beta = 0.5$ and $\gamma = 0$, RCSP becomes CCSP.

2.7. ReliefF

ReliefF [13] is a classical feature selection approach. Next we introduce its basic idea for binary classification.

Let x_i be the i -th feature, whose importance $w(x_i)$ is initialized to 0. ReliefF randomly selects a sample \mathbf{x} , and finds its k ($k = 10$ in this paper) nearest neighbors $H = \{\mathbf{h}_j\}_{j=1}^k$ in the same class, and also k nearest neighbors $M = \{\mathbf{m}_j\}_{j=1}^k$ in the other class. It then updates $w(x_i)$ by

$$w(x_i) = w(x_i) - \frac{1}{k} \sum_{j=1}^k \text{diff}(x_i, \mathbf{x}, \mathbf{h}_j) + \frac{1}{k} \sum_{j=1}^k \text{diff}(x_i, \mathbf{x}, \mathbf{m}_j), \quad (11)$$

where $\text{diff}(x_i, \mathbf{x}, \mathbf{x}')$ denotes the difference between samples \mathbf{x} and \mathbf{x}' in terms of feature x_i . (11) is very intuitive: the importance of x_i should be decreased with its ability to discriminate samples from the same class [$\text{diff}(x_i, \mathbf{x}, \mathbf{h})$], and increased with its ability to discriminate samples from different classes [$\text{diff}(x_i, \mathbf{x}, \mathbf{m})$].

In this paper, ReliefF terminates after 100 iterations, i.e., 100 randomly selected \mathbf{x} were used to compute the final $w(x_i)$. We then rank these $w(x_i)$ and select a few features corresponding to the largest $w(x_i)$.

2.8. Combined ReliefF (CReliefF)

The traditional ReliefF selects \mathbf{x} , H and M from only the target domain labeled samples. We propose a very simple TL extension of ReliefF, combined ReliefF (CReliefF), by selecting \mathbf{x} , H and M from labeled samples in both domains.

2.9. LDA

LDA is a popular linear classifier for binary classification. It assumes that the feature covariance matrices (not to be confused with the spatial covariance matrix of an EEG trial) from the two classes have full rank and are both equal to Σ_t . The classification for a new input \mathbf{x} is then

$$\text{sign}(\mathbf{w}\mathbf{x}^\top - \theta), \quad (12)$$

where

$$\mathbf{w} = \Sigma_t^{-1}(\bar{\mathbf{x}}_{t,1} - \bar{\mathbf{x}}_{t,-1}), \quad (13)$$

$$\theta = \frac{1}{2}\mathbf{w}(\bar{\mathbf{x}}_{t,1} + \bar{\mathbf{x}}_{t,-1}), \quad (14)$$

in which $\bar{\mathbf{x}}_{t,-1}$ and $\bar{\mathbf{x}}_{t,1}$ are the mean feature vector of Class -1 and Class 1 computed from the N_l target domain labeled samples, respectively.

2.10. Combined LDA (CLDA)

When N_l is small, the above LDA classifier may not be reliable. The combined LDA (CLDA) is a simple TL approach, which concatenates labeled samples from both the source domain and the target domain to train an LDA classifier. All samples from both domains are treated equally.

2.11. Weighted Adaptation Regularization (wAR)

Wu [44] proposed weighted adaptation regularization (wAR), a TL approach for offline cross-subject EEG classification. Though the original experiments were conducted for event-related potential classification, wAR can also be used for MI classification.

wAR learns a classifier f^* by minimizing the following regularized loss function:

$$\begin{aligned} f^* = \operatorname{argmin}_f & \sum_{n=1}^{N_s} w_s^n \ell(f(\mathbf{x}_s^n), y_s^n) + w_t \sum_{n=1}^{N_l} w_t^n \ell(f(\mathbf{x}_t^n), y_t^n) \\ & + \lambda_1 \|f\|_K^2 + \lambda_2 D_{f,K}(P_s(\mathbf{x}_s), P_t(\mathbf{x}_t)) \\ & + \lambda_3 D_{f,K}(P_s(\mathbf{x}_s|y_s), P_t(\mathbf{x}_t|y_t)) \end{aligned} \quad (15)$$

where ℓ is the classification loss, w_t is the overall weight of samples from the target subject, w_s^n and w_t^n are the weights for the n -th sample from the source subject and the target subject, respectively, K is a kernel function, $P_s(\mathbf{x}_s)$ and $P_t(\mathbf{x}_t)$ are the marginal probability distribution of features from the source subject and the target subject, respectively, $P_s(\mathbf{x}_s|y_s)$ and $P_t(\mathbf{x}_t|y_t)$ are the conditional probability distribution from the source subject and the target subject, respectively, and λ_1 , λ_2 and λ_3 are non-negative regularization parameters.

Briefly speaking, the five terms in (15) minimize the classification loss for the source subject, the classification loss for the target subject, the structural risk of the

classifier, the distance between the marginal probability distributions of the two subjects, and the distance between the conditional probability distributions of the two subjects, respectively.

Although it looks complicated, (15) has a closed-form solution when the squared loss $\ell(f(\mathbf{x}) - y) = (y - f(\mathbf{x}))^2$ is used [44].

2.12. Online wAR (OwAR)

Wu [44] also proposed online wAR (OwAR), a TL approach for online cross-subject EEG classification.

OwAR learns a classifier f^* , also by minimizing the regularized loss function in (15). The only difference is that now the kernel matrix K can only be computed from the N_s labeled source domain samples and N_l labeled target domain samples, but not the N_u unlabeled target domain samples, which are unavailable in online classification.

3. Experiments and Results

This section evaluates the offline cross-subject classification performances of different combinations of TL approaches on two MI datasets.

3.1. MI Datasets

Two MI datasets from BCI Competition IV¹ were used in this study. They were also used in our previous research [9, 10, 54].

In each experiment, the subject sat in front of a computer and performed visual cue based MI tasks, as shown in Figure 5. A fixation cross on the black screen ($t = 0$) prompted the subject to be prepared, and marked the start of a trial. After two seconds, a visual cue, which was an arrow pointing to a certain direction, was displayed for four seconds, during which the subject performed the instructed MI task. The visual cue disappeared at $t = 6$ second, and the MI also stopped. After a two-second break, the next trial started.

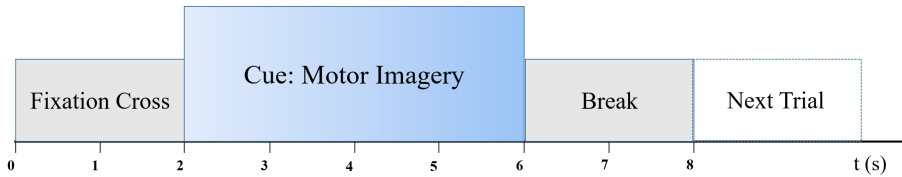


Figure 5: Timing scheme of the MI tasks.

The first dataset² (Dataset 1 [2]) consisted of seven healthy subjects. Each subject performed two types of MIs, selected from three classes: left-hand, right-hand, and

¹<http://www.bbc.de/competition/iv/>.

²http://www.bbc.de/competition/iv/desc_1.html.

foot. We used the 59-channel EEG data collected from the calibration phase, which included complete marker information. Each subject had 100 trials per class.

The second MI dataset³ (Dataset 2a) included nine healthy subjects. Each subject performed four different MIs: left-hand, right-hand, both feet, and tongue. We used the 22-channel EEG data and two classes of MIs (left-hand and right-hand) collected from the training phase. Each subject had 72 trials per class.

EEG data preprocessing steps were identical to those in [10]. A causal [8, 30] Hz band-pass filter was used to remove muscle artifacts, powerline noise, and DC drift. Next, we extracted EEG signals between [0.5, 3.5] seconds after the cue onset as our trials for both datasets.

3.2. Algorithms

We mainly compare the following 18 different algorithms, with various different configurations of TL components:

1. *CSP-LDA*, which uses only the target domain labeled data to design the CSP filters, and then trains an LDA classifier on the target domain labeled data. No source data is used at all, i.e., no TL is used at all.
2. *CSP-CLDA*, which uses only the target domain labeled data to design the CSP filters, and then trains a CLDA classifier by using labeled data from both domains, i.e., only the classifier uses a simple TL approach.
3. *CSP-wAR*, which uses only the target domain labeled data to design the CSP filters, and then trains a wAR classifier by using data from both domains, i.e., only the classifier uses a sophisticated TL approach.
4. *CCSP-LDA*, which concatenates labeled data from both domains to design the CCSP filters, and then trains an LDA classifier on target domain labeled data only, i.e., only spatial filtering uses a simple TL approach.
5. *CCSP-CLDA*, which concatenates labeled data from both domains to design the CCSP filters, and then trains a CLDA classifier also from the concatenated data, i.e., both spatial filtering and classification use a simple TL approach.
6. *CCSP-wAR*, which concatenates labeled data from both domains to design the CCSP filters, and then trains a wAR classifier also from the concatenated data, i.e., spatial filtering uses a simple TL approach, whereas classification uses a sophisticated TL approach.
7. *RCSP-LDA*, which uses labeled data from both domains to design the RCSP filters, and then trains an LDA classifier from the target domain labeled data only, i.e., spatial filtering uses a sophisticated TL approach, whereas classification does not use TL at all.
8. *RCSP-CLDA*, which uses labeled data from both domains to design the RCSP filters, and then trains a CLDA classifier also from this concatenated data, i.e., spatial filtering uses a sophisticated TL approach, whereas classification uses a simple TL approach.

³http://www.bbci.de/competition/iv/desc_2a.pdf.

9. *RCSP-wAR*, which uses labeled data from both domains to design the RCSP filters, and then trains a wAR classifier from this concatenated data, i.e., both spatial filtering and classification use a sophisticated TL approach.
10. *EA-CSP-LDA*, which performs EA before CSP-LDA.
11. *EA-CSP-CLDA*, which performs EA before CSP-CLDA, i.e., only the classifier uses a simple TL approach, after EA.
12. *EA-CSP-wAR*, which performs EA before CSP-wAR, i.e., only the classifier uses a sophisticated TL approach, after EA.
13. *EA-CCSP-LDA*, which performs EA before CCSP-LDA, i.e., only spatial filtering uses a simple TL approach, after EA.
14. *EA-CCSP-CLDA*, which performs EA before CCSP-CLDA, i.e., both spatial filtering and classification use a simple TL approach, after EA.
15. *EA-CCSP-wAR*, which performs EA before CCSP-wAR, i.e., spatial filtering uses a simple TL approach, whereas classification uses a sophisticated TL approach, after EA.
16. *EA-RCSP-LDA*, which performs EA before RCSP-LDA, i.e., only spatial filtering uses a sophisticated TL approach, after EA.
17. *EA-RCSP-CLDA*, which performs EA before RCSP-CLDA, i.e., spatial filtering uses a sophisticated TL approach, whereas classification uses a simple TL approach, after EA.
18. *EA-RCSP-wAR*, which performs EA before RCSP-wAR, i.e., both spatial filtering and classification use a sophisticated TL approach, after EA.

Additionally, there were nine PS based approaches, which replace EA in the nine EA based approaches by PS, respectively. A summary of the 27 algorithms is shown in Table 1.

Six (a typical number [34]) spatial filters were used in all CSP algorithms. $\beta = \gamma = 0.1$ were used in RCSP. $w_t = 10$, $\lambda_1 = 0.1$, $\lambda_2 = \lambda_3 = 10$ were used in wAR, as in [44, 48], except that w_t was increased from 2 to 10 because the combined source domain has much more labeled samples than the target domain. The source code is available at <https://github.com/drwuHUST/TLBCI>.

By comparing between different pairs of the above algorithms, we can individually study the effect of TL in different components of Figure 2.

3.3. Experimental Settings and Results

For each dataset, we sequentially selected one subject as the target subject and all remaining ones as the source subjects, i.e., we performed cross-subject evaluations. As in [10], we combined all source subjects as a single source domain, and performed the corresponding TL. This procedure was repeated for each subject, so that each one became the target subject once.

The number of randomly selected labeled samples in the target domain (N_l) increased from zero to 20, with a step of 4. Because there was randomness involved, we repeated this process 30 times and report the average results.

Note that for algorithms whose spatial filtering component did not involve TL, e.g., those with *CSP*-, when $N_l = 0$, no CSP filters can be trained, and hence no model can

Table 1: Summary of the 27 algorithms with various degrees of TL.

Algorithm	Data Alignment	Spatia Filtering		Classifier	
		Simple TL	Sophisticated TL	Simple TL	Sophisticated TL
CSP-LDA	–	–	–	–	–
CSP-CLDA	–	–	–	✓	–
CSP-wAR	–	–	–	–	✓
CCSP-LDA	–	✓	–	–	–
CCSP-CLDA	–	✓	–	✓	–
CCSP-wAR	–	✓	–	–	✓
RCSP-LDA	–	–	✓	–	–
RCSP-CLDA	–	–	✓	✓	–
RCSP-wAR	–	–	✓	–	✓
EA-CSP-LDA	✓	–	–	–	–
EA-CSP-CLDA	✓	–	–	✓	–
EA-CSP-wAR	✓	–	–	–	✓
EA-CCSP-LDA	✓	✓	–	–	–
EA-CCSP-CLDA	✓	✓	–	✓	–
EA-CCSP-wAR	✓	✓	–	–	✓
EA-RCSP-LDA	✓	–	✓	–	–
EA-RCSP-CLDA	✓	–	✓	✓	–
EA-RCSP-wAR	✓	–	✓	–	✓
PS-CSP-LDA	✓	–	–	–	–
PS-CSP-CLDA	✓	–	–	✓	–
PS-CSP-wAR	✓	–	–	–	✓
PS-CCSP-LDA	✓	✓	–	–	–
PS-CCSP-CLDA	✓	✓	–	✓	–
PS-CCSP-wAR	✓	✓	–	–	✓
PS-RCSP-LDA	✓	–	✓	–	–
PS-RCSP-CLDA	✓	–	✓	✓	–
PS-RCSP-wAR	✓	–	✓	–	✓

be built. All other algorithms used TL in CSP, and hence the source domain labeled data can be used to train the CSP filters even when $N_l = 0$. Similarly, for algorithms whose classifier did not involve TL, e.g., those with *-LDA*, when $N_l = 0$, no LDA classifier can be trained.

Note also that since we consider offline classification, all unlabeled samples in the target domain are known, and can be used in EA, PS and wAR. There is no data leakage here.

The cross-subject classification accuracies, averaged over 30 random runs, are shown in Figure 6. The average performances over all subjects are shown in the last panel of each subfigure. To ensure that the curves are distinguishable, we omitted the curves from the nine PS based algorithms, which were very similar to their EA counterparts.

3.4. The General Effect of TL

In Figure 6, by comparing CSP-LDA, which did not use TL at all, with the other 17 algorithms, which used simple or sophisticated TL in one or more components of Figure 2, we can see that when N_l was small, TL almost always resulted in better performance, no matter how much TL was used. However, when N_l increased, CSP-LDA gradually outperformed certain simple TL approaches, e.g., CSP-CLDA and CCSP-CLDA, whereas sophisticated TL approaches, e.g., EA-RCSP-wAR, almost always outperformed CSP-LDA. These results suggest that sophisticated TL may always be beneficial.

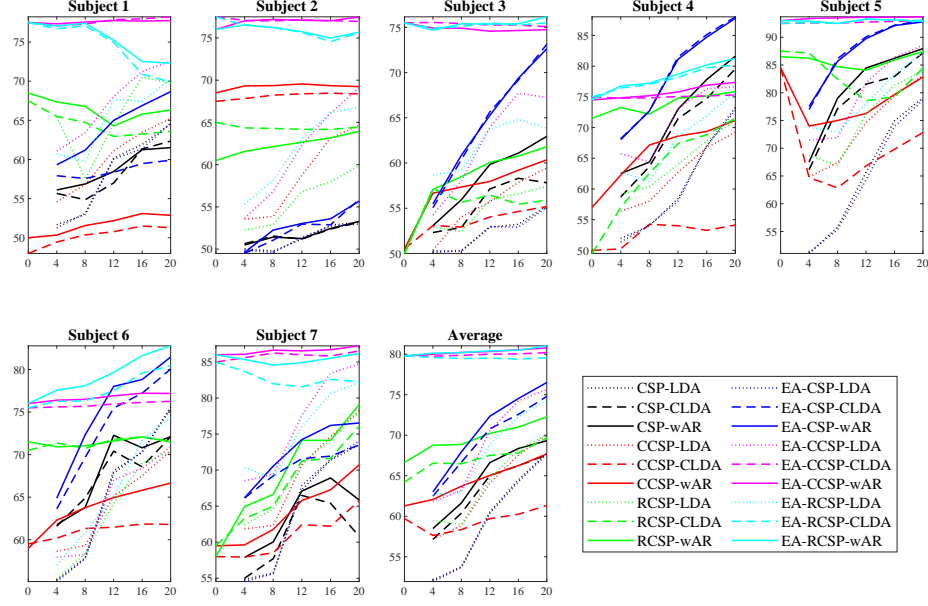
To quantitatively study the general effect of TL, we computed the mean classification accuracies of the 27 approaches when N_l increased from 4 to 20 (we did not use $N_l = 0$ because certain approaches did not work in this case), and compared them with that of CSP-LDA. The results are shown in Table 2. We also performed paired *t*-tests to verify if the performance improvements over CSP-LDA were statistically significant ($\alpha = 0.05$), and marked the insignificant ones by an underline. Table 2 confirms again that generally more sophisticated TL approaches achieved larger performance improvements.

3.5. The Effect of Data Alignment

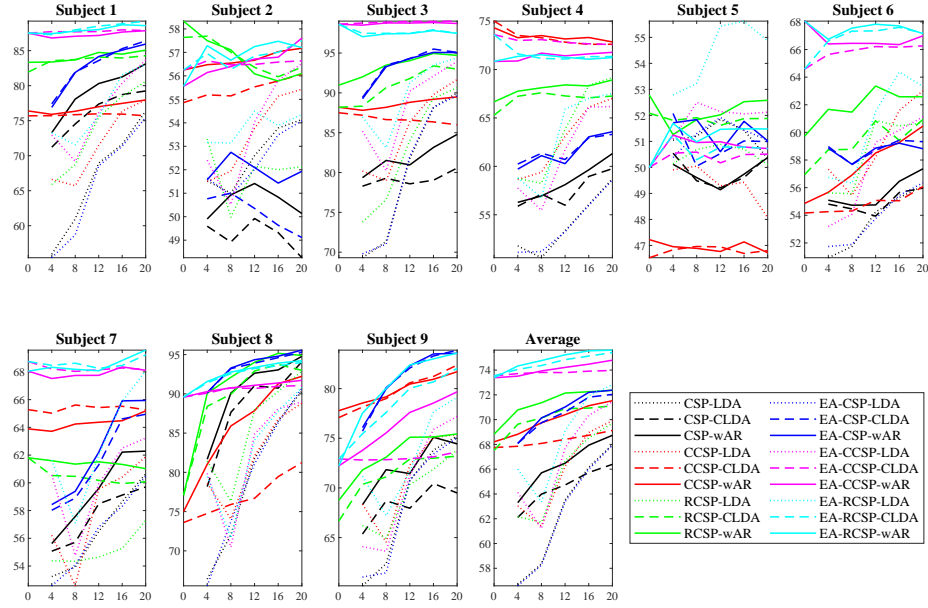
In Figure 6, comparing algorithms without EA and their counterparts with EA, e.g., CSP-CLDA and EA-CSP-CLDA, we can observe that every EA version almost always significantly outperformed its non-EA counterpart. Similar observations can also be made for PS. These results suggest that a data alignment approach such as EA or PS should always be included as a TL preprocessing step in a BCI system.

To quantitatively verify the above conclusion, we also show the mean classification accuracies of algorithms without and with EA/PS in Table 3. Clearly, EA and PS significantly improved the classification accuracies when TL is used in at least one component of spatial filtering and classification, especially on Dataset 1.

Interestingly, when CSP-LDA was used, i.e., no TL was used at all in spatial filtering and classification, EA/PS slightly reduced the classification performance. We were not able to find an explanation for this; however, when no TL will be performed, there is no point to align EEG trials from different subjects. So, this negative transfer will not happen in practice, and should not be a concern.



(a)



(b)

Figure 6: Offline cross-subject classification accuracies (vertical axis) on the MI datasets, with different N_l (horizontal axis). (a) Dataset 1; (b) Dataset 2a.

Table 2: Offline cross-subject classification accuracies (mean \pm std) of different TL approaches, and their improvements over CSP-LDA. Performance improvements not statistically significant ($\alpha = 0.05$) are marked with an underline.

Algorithm	Dataset 1		Dataset 2a	
	Accuracy (%)	Improvement (%)	Accuracy (%)	Improvement (%)
CSP-LDA	59.75 \pm 6.74	–	62.54 \pm 4.88	–
CSP-CLDA	63.27 \pm 4.37	5.91	64.59 \pm 1.67	3.27
CSP-wAR	64.88 \pm 4.65	8.60	66.43 \pm 2.12	6.22
CCSP-LDA	63.54 \pm 5.52	6.35	65.91 \pm 3.67	5.39
CCSP-CLDA	59.45 \pm 1.48	<u>-0.49</u>	68.44 \pm 0.51	9.43
CCSP-wAR	64.95 \pm 2.18	8.72	70.32 \pm 1.08	12.44
RCSP-LDA	64.28 \pm 5.01	7.59	65.76 \pm 3.65	5.15
RCSP-CLDA	67.60 \pm 1.29	13.15	70.54 \pm 0.63	12.78
RCSP-wAR	70.22 \pm 1.49	17.54	71.78 \pm 0.68	14.77
EA-CSP-LDA	59.57 \pm 6.72	-0.29	62.43 \pm 4.89	<u>-0.18</u>
EA-CSP-CLDA	69.46 \pm 4.91	16.27	70.46 \pm 1.62	12.66
EA-CSP-wAR	70.87 \pm 5.43	18.61	70.76 \pm 1.76	13.14
EA-CCSP-LDA	69.09 \pm 6.32	15.64	66.97 \pm 4.28	7.08
EA-CCSP-CLDA	79.97 \pm 0.17	33.85	73.84 \pm 0.10	18.07
EA-CCSP-wAR	80.37 \pm 0.30	34.52	74.19 \pm 0.50	18.62
EA-RCSP-LDA	68.24 \pm 5.31	14.21	68.64 \pm 3.99	9.75
EA-RCSP-CLDA	79.51 \pm 0.08	33.08	74.76 \pm 0.55	19.54
EA-RCSP-wAR	80.45 \pm 0.35	34.66	75.10 \pm 0.54	20.08
PS-CSP-LDA	59.58 \pm 6.73	-0.28	62.47 \pm 4.90	<u>-0.12</u>
PS-CSP-CLDA	71.51 \pm 5.26	19.69	70.49 \pm 1.59	12.71
PS-CSP-wAR	71.89 \pm 5.17	20.33	70.85 \pm 1.70	13.29
PS-CCSP-LDA	67.59 \pm 5.72	13.13	66.48 \pm 4.17	6.29
PS-CCSP-CLDA	78.35 \pm 0.18	31.14	73.87 \pm 0.14	18.11
PS-CCSP-wAR	79.15 \pm 0.14	32.48	74.67 \pm 0.47	19.39
PS-RCSP-LDA	68.92 \pm 5.25	15.36	68.02 \pm 3.89	8.77
PS-RCSP-CLDA	79.15 \pm 0.13	32.48	74.22 \pm 0.66	18.68
PS-RCSP-wAR	79.56 \pm 0.17	33.17	74.68 \pm 0.70	19.40

Table 3: Offline cross-subject classification accuracies (mean \pm std) of algorithms without and with EA/PS, and the improvements of the latter over the former. Performance improvements not statistically significant ($\alpha = 0.05$) are marked with an underline.

Dataset	Algorithm	w/o EA (%)	w/ EA (%)	Imp. (%)	w/o PS (%)	w/ PS (%)	Imp. (%)
1	CSP-LDA	59.75 \pm 6.74	59.57 \pm 6.72	-0.29	59.75 \pm 6.74	59.58 \pm 6.73	-0.28
	CSP-CLDA	63.27 \pm 4.37	69.46 \pm 4.91	9.79	63.27 \pm 4.37	71.51 \pm 5.26	13.02
	CSP-wAR	64.88 \pm 4.65	70.87 \pm 5.43	9.22	64.88 \pm 4.65	71.89 \pm 5.17	10.80
	CCSP-LDA	63.54 \pm 5.52	69.09 \pm 6.32	8.74	63.54 \pm 5.52	67.59 \pm 5.72	6.37
	CCSP-CLDA	59.45 \pm 1.48	79.97 \pm 0.17	34.51	59.45 \pm 1.48	78.35 \pm 0.18	31.78
	CCSP-wAR	64.95 \pm 2.18	80.37 \pm 0.30	23.74	64.95 \pm 2.18	79.15 \pm 0.14	21.86
	RCSP-LDA	64.28 \pm 5.01	68.24 \pm 5.31	6.16	64.28 \pm 5.01	68.92 \pm 5.25	7.22
	RCSP-CLDA	67.60 \pm 1.29	79.51 \pm 0.08	17.61	67.60 \pm 1.29	79.15 \pm 0.13	17.08
	RCSP-wAR	70.22 \pm 1.49	80.45 \pm 0.35	14.56	70.22 \pm 1.49	79.56 \pm 0.17	13.29
2a	CSP-LDA	62.54 \pm 4.88	62.43 \pm 4.89	<u>-0.18</u>	62.54 \pm 4.88	62.47 \pm 4.90	<u>-0.12</u>
	CSP-CLDA	64.59 \pm 1.67	70.46 \pm 1.62	9.09	64.59 \pm 1.67	70.49 \pm 1.59	9.14
	CSP-wAR	66.43 \pm 2.12	70.76 \pm 1.76	6.52	66.43 \pm 2.12	70.85 \pm 1.70	6.66
	CCSP-LDA	65.91 \pm 3.67	66.97 \pm 4.28	1.60	65.91 \pm 3.67	66.48 \pm 4.17	<u>0.86</u>
	CCSP-CLDA	68.44 \pm 0.51	73.84 \pm 0.10	7.89	68.44 \pm 0.51	73.87 \pm 0.14	7.93
	CCSP-wAR	70.32 \pm 1.08	74.19 \pm 0.50	5.49	70.32 \pm 1.08	74.67 \pm 0.47	6.18
	RCSP-LDA	65.76 \pm 3.65	68.64 \pm 3.99	4.38	65.76 \pm 3.65	68.02 \pm 3.89	3.44
	RCSP-CLDA	70.54 \pm 0.63	74.76 \pm 0.55	5.99	70.54 \pm 0.63	74.22 \pm 0.66	5.22
	RCSP-wAR	71.78 \pm 0.68	75.10 \pm 0.54	4.62	71.78 \pm 0.68	74.68 \pm 0.70	4.03

3.6. The Effect of TL in Spatial Filtering

In Figure 6, comparing algorithms without TL in spatial filtering (CSP), with simple TL in spatial filtering (CCSP), and with sophisticated TL in spatial filtering (RCSP), e.g., CSP-CLDA, CCSP-CLDA and RCSP-CLDA, we can observe that simple TL in spatial filtering may not always work (e.g., CCSP-CLDA had worse performance than CSP-CLDA on Dataset 1, but better performance on Dataset 2a), but sophisticated TL in spatial filtering was almost always beneficial (e.g., RCSP-CLDA outperformed both CSP-CLDA and CCSP-CLDA on both datasets). So, sophisticated TL approaches, such as RCSP, should be used in spatial filtering in a BCI system.

To quantitatively verify the above conclusion, we also show the mean classification accuracies of algorithms without and with TL in spatial filtering in Table 4. Clearly, RCSP (sophisticated TL in spatial filtering) always outperformed the corresponding CSP (no TL in spatial filtering) and CCSP (simple TL in spatial filtering) versions.

Table 4: The effect of TL in spatial filtering. Performance improvements not statistically significant ($\alpha = 0.05$) are marked with an underline.

Dataset	Algorithm	No TL	Simple TL		Sophisticated TL	
		CSP	CCSP	Imp. (%)	RCSP	Imp. (%)
1	CSP-LDA	59.75±6.74	63.54±5.52	6.35	64.28±5.01	7.59
	CSP-CLDA	63.27±4.37	59.45±1.48	-6.04	67.60±1.29	6.84
	CSP-wAR	64.88±4.65	64.95±2.18	<u>0.11</u>	70.22±1.49	8.23
	EA-CSP-LDA	59.57±6.72	69.09±6.32	15.98	68.24±5.31	14.55
	EA-CSP-CLDA	69.46±4.91	79.97±0.17	15.12	79.51±0.08	14.46
	EA-CSP-wAR	70.87±5.43	80.37±0.30	13.41	80.45±0.35	13.53
	PS-CSP-LDA	59.58±6.73	67.59±5.72	13.44	68.92±5.25	15.68
	PS-CSP-CLDA	71.51±5.26	78.35±0.18	9.56	79.15±0.13	10.68
	PS-CSP-wAR	71.89±5.17	79.15±0.14	10.10	79.56±0.17	10.66
2a	CSP-LDA	62.54±4.88	65.91±3.67	5.39	65.76±3.65	5.15
	CSP-CLDA	64.59±1.67	68.44±0.51	5.96	70.54±0.63	9.21
	CSP-wAR	66.43±2.12	70.32±1.08	5.86	71.78±0.68	8.06
	EA-CSP-LDA	62.43±4.89	66.97±4.28	7.28	68.64±3.99	9.95
	EA-CSP-CLDA	70.46±1.62	73.84±0.10	4.80	74.76±0.55	6.11
	EA-CSP-wAR	70.76±1.76	74.19±0.50	4.84	75.10±0.54	6.13
	PS-CSP-LDA	62.47±4.90	66.48±4.17	6.42	68.02±3.89	8.90
	PS-CSP-CLDA	70.49±1.59	73.87±0.14	4.79	74.22±0.66	5.29
	PS-CSP-wAR	70.85±1.70	74.67±0.47	5.39	74.68±0.70	5.40

3.7. The Effect of TL in Feature Selection

Assume $2f$ spatial filters are needed. Then, as introduced in Section 2.4, in traditional CSP, f of them are the leading eigenvectors of $(\bar{C}^N)^{-1}\bar{C}^P$, and the other f are the leading eigenvectors of $(\bar{C}^P)^{-1}\bar{C}^N$, where \bar{C}^P and \bar{C}^N are the mean covariance matrices of the positive and negative classes, respectively. $f = 3$ is typically used in the literature.

In this subsection, in order to show the effect of TL in feature selection, we use $f = 10$ to extract 20 CSP filters, compute the 20 corresponding features in (8), and then use different versions of ReliefF to select the best six among them. More specifically, without data alignment, we compared the following algorithms:

1. *CSP6-LDA*, which is identical to *CSP-LDA* in previous subsections. Here we add ‘6’ to emphasize that it uses six CSP filters, obtained from the leading eigenvectors.
2. *CSP20-ReliefF6-LDA*, which uses the traditional CSP algorithm to extract 20 spatial filters, compute the 20 corresponding features in (8), and then use ReliefF to select the best six from them. ReliefF uses the target domain labeled data only, i.e., no TL is used.
3. *CSP20-CReliefF6-LDA*, which uses the traditional CSP to extract 20 filters, compute the 20 corresponding features in (8), and then use CReliefF to select the best six from them. CReliefF uses labeled data from both domains, so there is TL.

LDA above can also be replaced by wAR, and CSP by RCSP. So, there could be 12 different configurations. Additionally, EA can also be added before each algorithm. So, there are a total of 24 different algorithms.

The cross-subject classification results of the 24 algorithms are shown in Table 5. When CReliefF was used to select the best six spatial filters from the 20 candidates (CSP20→CReliefF6), the resulting classification performance was generally better than using ReliefF directly (CSP20→ReliefF6), i.e., TL could be helpful in feature selection. However, using the six leading eigenvectors in CSP (CSP6) generally gave the best performance, justifying the common practice in the literature.

In summary, we have shown that if feature selection must be performed, then using TL may improve the performance; however, when CSP filters are used, using the leading eigenvectors is good enough, and we can safely omit feature selection.

3.8. The Effect of TL in the Classifier

In Figure 6, comparing algorithms with simple and sophisticated TL in the classifier, e.g., CCSP-CLDA and CCSP-wAR, we can observe that sophisticated TL in the classifier almost always outperformed simple TL, regardless of whether TL was used in other components or not. So, sophisticated TL approaches, such as wAR, should be used in the classifier in a BCI system.

To quantitatively verify the above conclusion, we also show the mean classification accuracies of algorithms without and with TL in the classifier in Table 6. Clearly, on average wAR (sophisticated TL in the classifier) always outperformed CLDA (simple TL in the classifier).

Table 5: The effect of TL in feature selection. Performance improvements not statistically significant ($\alpha = 0.05$) are marked with an underline.

Dataset	Algorithm	No TL		TL	
		CSP6	CSP20→ReliefF6	CSP20→CReliefF6	Imp. (%)
1	CSP-LDA	59.91±6.72	58.91±6.47	59.74±6.23	1.40
	CSP-wAR	64.21±5.14	61.20±5.54	63.86±5.22	4.36
	RCSP-LDA	64.74±5.36	61.38±5.97	63.89±5.50	4.09
	RCSP-wAR	70.85±1.08	64.67±3.55	70.71±0.96	9.35
	EA-CSP-LDA	59.79±6.61	58.02±5.79	60.75±6.69	4.71
	EA-CSP-wAR	70.48±5.66	65.68±5.93	71.26±6.35	8.50
	EA-RCSP-LDA	69.52±5.25	63.51±5.89	68.11±6.10	7.24
	EA-RCSP-wAR	81.63±0.91	72.78±3.88	81.45±1.01	11.92
2a	CSP-LDA	62.32±5.63	61.86±5.51	62.82±4.98	1.55
	CSP-wAR	66.21±2.50	64.72±3.12	65.29±2.49	0.89
	RCSP-LDA	65.35±4.11	62.97±5.12	64.78±4.17	2.88
	RCSP-wAR	71.58±0.73	68.08±2.40	70.79±0.98	3.98
	EA-CSP-LDA	62.28±5.66	61.24±5.70	61.43±4.60	<u>0.31</u>
	EA-CSP-wAR	70.50±2.38	69.11±3.11	68.13±1.67	-1.42
	EA-RCSP-LDA	68.50±4.13	64.19±4.68	62.37±3.94	-2.83
	EA-RCSP-wAR	75.00±0.59	72.42±1.63	69.55±0.38	-3.96

Interestingly, when EA or PS was used, the performance improvement of wAR over CLDA became smaller, because EA or PS reduced the discrepancy between the source and target domain data, and hence made classification easier.

Table 6: The effect of TL in the classifier. Performance improvements not statistically significant ($\alpha = 0.05$) are marked with an underline.

Dataset	Algorithm	No TL	Simple TL		Sophisticated TL	
		LDA	CLDA	Imp. (%)	wAR	Imp. (%)
1	CSP-LDA	59.75±6.74	63.27±4.37	5.91	64.88±4.65	8.60
	CCSP-LDA	63.54±5.52	59.45±1.48	-6.43	64.95±2.18	<u>2.23</u>
	RCSP-LDA	64.28±5.01	67.60±1.29	5.17	70.22±1.49	9.25
	EA-CSP-LDA	59.57±6.72	69.46±4.91	16.61	70.87±5.43	18.96
	EA-CCSP-LDA	69.09±6.32	79.97±0.17	15.74	80.37±0.30	16.33
	EA-RCSP-LDA	68.24±5.31	79.51±0.08	16.51	80.45±0.35	17.90
	PS-CSP-LDA	59.58±6.73	71.51±5.26	20.02	71.89±5.17	20.67
	PS-CCSP-LDA	67.59±5.72	78.35±0.18	15.92	79.15±0.14	17.11
	PS-RCSP-LDA	68.92±5.25	79.15±0.13	14.84	79.56±0.17	15.44
2a	CSP-LDA	62.54±4.88	64.59±1.67	3.27	66.43±2.12	6.22
	CCSP-LDA	65.91±3.67	68.44±0.51	3.83	70.32±1.08	6.69
	RCSP-LDA	65.76±3.65	70.54±0.63	7.26	71.78±0.68	9.16
	EA-CSP-LDA	62.43±4.89	70.46±1.62	12.86	70.76±1.76	13.35
	EA-CCSP-LDA	66.97±4.28	73.84±0.10	10.26	74.19±0.50	10.77
	EA-RCSP-LDA	68.64±3.99	74.76±0.55	8.92	75.10±0.54	9.41
	PS-CSP-LDA	62.47±4.90	70.49±1.59	12.85	70.85±1.70	13.42
	PS-CCSP-LDA	66.48±4.17	73.87±0.14	11.12	74.67±0.47	12.32
	PS-RCSP-LDA	68.02±3.89	74.22±0.66	9.11	74.68±0.70	9.78

4. Discussion

The section discusses the TL pipeline in offline cross-subject MI classification using deep learning, online cross-subject classification, and offline cross-session classification.

4.1. Offline Cross-Subject Classification Using Deep Learning

The previous section verified the effectiveness of TL in a traditional machine learning pipeline. Deep learning has made significant breakthroughs in many fields, including EEG-based BCIs. This subsection considers the TL pipeline in offline cross-subject MI classification using deep learning models.

Two popular convolutional neural network (CNN) classifiers, EEGNet [17] and ShallowCNN [39], were used in our experiments. EEGNet is a compact convolutional network with only about 1,000 parameters (the number may change slightly according to the nature of the task) for EEG-based BCIs. It introduces depthwise and separable convolutions into the construction of EEG-specific CNNs, which encapsulate well-known EEG feature extraction concepts and simultaneously reduce the number of model parameters. ShallowCNN has a very shallow architecture, consisting of a convolutional block and a classification block. The convolutional block is specially designed to handle EEG signals.

Because CNN models perform simultaneously spatial filtering, feature engineering and classification, and their computational cost is much higher than traditional machine learning models, we only compared the performances with and without EA in Figure 2. More specifically, we considered offline unsupervised cross-subject classification, i.e., all samples from the target subject were unlabeled ($N_l = 0$), and all samples from the source subjects were combined and partitioned into 80% training and 20% validation (for early stopping). We used Adam optimizer, cross entropy loss, and batch size 32. The experiments were repeated 15 times for each target subject.

The results are shown in Table 7. Clearly, using EA can improve the classification performance of both deep learning models, especially on Dataset 1. These results are consistent with a more comprehensive study in [14], which shows that EA generally benefits deep learning classification of movement and motor imagery, P300, and error related negativity.

Table 7: The effect of EA in deep learning. Performance improvements not statistically significant ($\alpha = 0.05$) are marked with an underline.

Dataset	Model	w/o EA (%)	w/ EA (%)	Improvement (%)
1	EEGNet	59.35±4.80	70.00±8.14	17.94
	ShallowCNN	62.85±7.47	73.92±8.48	17.61
2a	EEGNet	72.71±3.62	75.84±4.61	<u>4.30</u>
	ShallowCNN	68.00±3.43	73.46±1.76	3.59

4.2. Online Cross-Subject Classification

All previous results considered offline cross-subject MI classification. It is also interesting to study if the TL pipeline in Figure 2 can be used in online cross-subject MI classification.

To this end, we make sure EA and PS use only the available labeled target domain samples in computing the reference matrix and performing data alignment in the target domain. We also replace wAR by OwAR [44], which does not make use of offline unlabeled samples in the target domain in classifier training.

The online cross-subject classification results are shown in Figure 7 and Table 8. Generally, all observations made from offline cross-subject classification in the previous section, e.g., considering TL in more components of Figure 2 benefits the perfor-

mance more, and data alignment is very important to subsequent TL, still hold in online cross-subject classification.

Comparing Tables 2 and 8 shows that the offline classification performances were generally slightly better than their online counterparts, which is intuitive, as offline classification makes use of the unlabeled target domain samples, which provides extra information in EA, PS and wAR.

4.3. Offline Cross-Session Classification

It is well-known that EEG signals are non-stationary [19], i.e., EEG responses to the same stimulus from the same subject in different sessions are usually varying. This subsection evaluates how the proposed TL pipeline can be used to handle EEG non-stationarity in cross-session classification.

In Dataset 2a, each of the nine subjects had two sessions (training and evaluation), collected on different days. For each subject, we used the training session as the source domain, and the evaluation session as the target domain. Other experimental settings were identical to those in previous subsections, except that we used $w_t = 2$ in wAR, as in cross-session TL the number of labeled source domain samples was much smaller than that in cross-subject TL.

The results are shown in Figure 8. Some subjects, e.g., Subjects 1, 3, 7, 8 and 9, demonstrated very stable classification performance when N_l increased, indicating that their EEG signals were quite stationary, at least in the two experimental sessions. However, the remaining four subjects’s EEG signals were more non-stationary, and hence the classification performance had large variations.

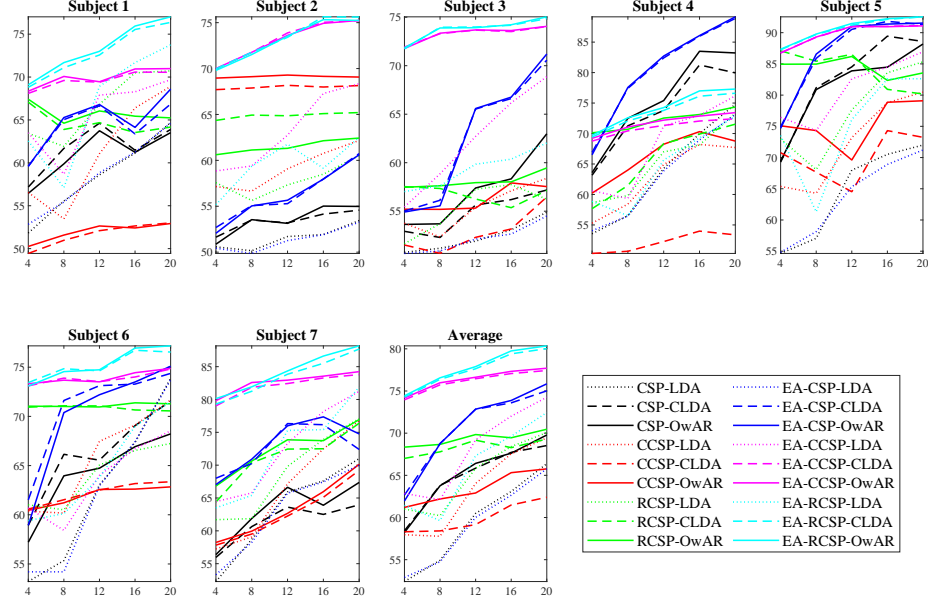
The average classification results are shown in Table 9. EA-CCSP-wAR, which integrates data alignment and TL in two components (spatial filtering and classification), achieved the best average performance. EA-RCSP-wAR, which was the best performer in cross-subject transfers in the previous section, was slightly worse, but still better than the other 16 approaches with or without TL. On average, almost all approaches with EA outperformed their counterparts without EA, suggesting again the importance and necessity of explicitly adding a data alignment block before TL.

In summary, TL is also effective in handling non-stationarity of EEG signals in cross-session MI classification, and considering TL in more components of the classification pipeline is generally more beneficial.

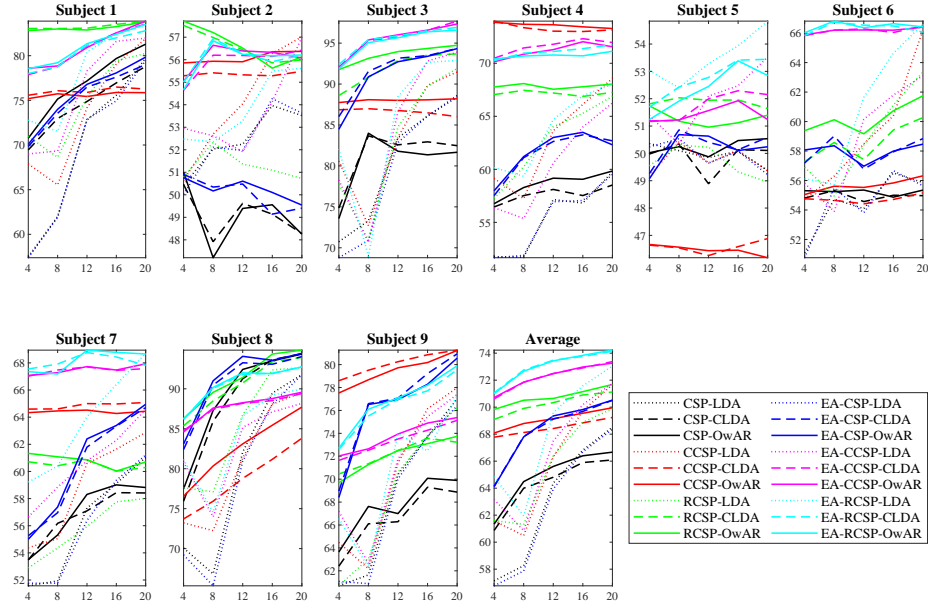
5. Conclusions and Future Research

Transfer learning has been widely used in MI-based BCIs to reduce the calibration effort for a new subject, and demonstrated promising performance. While a closed-loop MI-based BCI system, after EEG signal acquisition and temporal filtering, includes spatial filtering, feature engineering, and classification blocks before sending out the control signal to an external device, previous approaches only considered TL in one or two such components.

This paper proposes that TL could be considered in all three components, and it is also very important to specifically add a data alignment component before spatial filtering to make the source domain and target domain data more consistent. Offline and online classification experiments on two MI datasets verified that:



(a)



(b)

Figure 7: Online cross-subject classification accuracies (vertical axis) on the MI datasets, with different N_l (horizontal axis). (a) Dataset 1; (b) Dataset 2a.

Table 8: Online cross-subject classification accuracies (mean \pm std) of different TL approaches, and their improvements over CSP-LDA. Performance improvements not statistically significant ($\alpha = 0.05$) are marked with an underline.

Algorithm	Dataset 1		Dataset 2a	
	Accuracy (%)	Improvement (%)	Accuracy (%)	Improvement (%)
CSP-LDA	59.46 \pm 5.75	–	63.02 \pm 5.09	–
CSP-CLDA	64.87 \pm 4.03	9.10	64.33 \pm 2.11	<u>2.08</u>
CSP-OwAR	65.16 \pm 4.45	9.59	64.90 \pm 2.16	2.98
CCSP-LDA	63.35 \pm 5.37	6.55	65.96 \pm 4.90	4.66
CCSP-CLDA	59.95 \pm 1.87	<u>0.83</u>	68.48 \pm 0.58	8.66
CCSP-OwAR	63.48 \pm 1.98	6.76	69.10 \pm 0.72	9.66
RCSP-LDA	65.11 \pm 4.38	9.50	65.61 \pm 4.00	4.12
RCSP-CLDA	68.31 \pm 0.96	14.89	70.27 \pm 0.81	11.51
RCSP-OwAR	69.35 \pm 0.86	16.64	70.76 \pm 0.69	12.29
EA-CSP-LDA	59.22 \pm 5.37	<u>-0.41</u>	62.73 \pm 5.20	-0.47
EA-CSP-CLDA	70.58 \pm 5.00	18.70	68.26 \pm 2.49	8.31
EA-CSP-OwAR	70.66 \pm 5.51	18.83	68.32 \pm 2.56	8.41
EA-CCSP-LDA	68.09 \pm 5.43	14.52	66.69 \pm 4.61	5.83
EA-CCSP-CLDA	76.13 \pm 1.38	28.03	72.25 \pm 1.07	14.64
EA-CCSP-OwAR	76.36 \pm 1.39	28.43	72.26 \pm 1.02	14.66
EA-RCSP-LDA	66.10 \pm 5.43	11.16	68.20 \pm 4.67	8.23
EA-RCSP-CLDA	77.55 \pm 2.33	30.42	73.04 \pm 1.22	15.90
EA-RCSP-OwAR	77.80 \pm 2.41	30.84	73.03 \pm 1.27	15.89
PS-CSP-LDA	59.23 \pm 5.53	-0.38	62.75 \pm 5.23	-0.43
PS-CSP-CLDA	71.45 \pm 4.84	20.17	69.04 \pm 2.32	9.55
PS-CSP-OwAR	71.26 \pm 5.33	19.84	68.96 \pm 2.48	9.43
PS-CCSP-LDA	67.14 \pm 5.22	12.91	67.04 \pm 3.66	6.39
PS-CCSP-CLDA	76.25 \pm 1.13	28.23	72.47 \pm 1.10	14.99
PS-CCSP-OwAR	76.73 \pm 1.16	29.05	72.54 \pm 1.15	15.10
PS-RCSP-LDA	67.60 \pm 5.10	13.69	67.40 \pm 4.15	6.95
PS-RCSP-CLDA	76.62 \pm 1.16	28.86	72.69 \pm 1.33	15.34
PS-RCSP-OwAR	77.02 \pm 1.07	29.54	72.75 \pm 1.30	15.44

Table 9: Offline cross-session classification accuracies (mean \pm std) of different TL approaches, and their improvements over CSP-LDA. All performance improvements were statistically significant ($\alpha = 0.05$).

Algorithm	Accuracy (%)	Improvement (%)
CSP-LDA	62.30 \pm 5.03	–
CSP-CLDA	69.03 \pm 2.30	10.81
CSP-wAR	70.01 \pm 2.24	12.38
CCSP-LDA	67.87 \pm 3.39	8.95
CCSP-CLDA	72.44 \pm 0.18	16.27
CCSP-wAR	74.10 \pm 0.17	18.95
RCSP-LDA	66.14 \pm 3.18	6.16
RCSP-CLDA	72.68 \pm 0.45	16.66
RCSP-wAR	72.80 \pm 0.34	16.85
EA-CSP-LDA	62.00 \pm 5.13	-0.48
EA-CSP-CLDA	70.98 \pm 2.00	13.93
EA-CSP-wAR	71.22 \pm 2.04	14.32
EA-CCSP-LDA	67.88 \pm 3.79	8.95
EA-CCSP-CLDA	74.87 \pm 0.17	20.17
EA-CCSP-wAR	75.56 \pm 0.05	21.29
EA-RCSP-LDA	67.44 \pm 3.18	8.26
EA-RCSP-CLDA	74.10 \pm 0.48	18.94
EA-RCSP-wAR	75.17 \pm 0.24	20.66

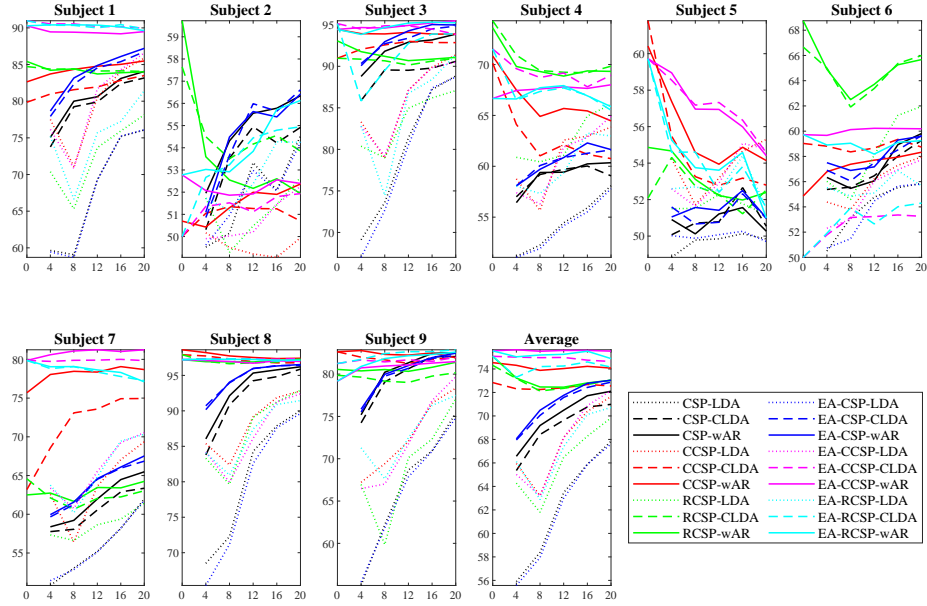


Figure 8: Offline cross-session classification accuracies (vertical axis) on Dataset 2a, with different N_l (horizontal axis).

1. Generally, using TL in different components of Figure 2 can achieve better classification performance than not using it, in both cross-subject and cross-session classification, for both online and offline classification.
2. Generally, a more sophisticated TL approach outperforms a simple one.
3. Data alignment is a very important preprocessing step in TL. It benefits both traditional machine learning and deep learning.
4. TL in different components of Figure 2 could be complementary to each other, so integrating them can further improve the classification performance.

The following directions will be considered in our future research:

1. Compared with other components, not enough attention has been paid to TL in feature engineering of BCI systems. We will develop more sophisticated TL approaches for feature engineering in the future, and also other components in Figure 2.
2. This paper considers only binary MI classification problems in BCIs. We will extend the analysis to other BCI classification paradigms, e.g., event-related potentials and steady-state visual evoked potentials, and also BCI regression problems, e.g., driver drowsiness estimation [5, 47] and user reaction-time estimation [49]. Furthermore, we will also consider TL in multi-class classification.
3. It has been shown [46, 48] that integrating TL with active learning [25] in the classifier can further improve the offline classification performance. It is interesting to study if TL and active learning can be integrated in other components of the BCI system, e.g., spatial filtering and feature engineering.

References

- [1] H. Albalawi, X. Song, A study of kernel CSP-based motor imagery brain computer interface classification, in: Proc. IEEE Signal Processing in Medicine and Biology Symposium, New York City, NY, 1–4, 2012.
- [2] B. Blankertz, G. Dornhege, M. Krauledat, K. R. Muller, G. Curio, The non-invasive Berlin Brain-Computer Interface: Fast acquisition of effective performance in untrained subjects, *NeuroImage* 37 (2) (2007) 539–550.
- [3] B. Blankertz, R. Tomioka, S. Lemm, M. Kawanabe, K. R. Muller, Optimizing Spatial filters for Robust EEG Single-Trial Analysis, *IEEE Signal Processing Magazine* 25 (1) (2008) 41–56.
- [4] L.-L. Chen, A. Zhang, X.-G. Lou, Cross-subject driver status detection from physiological signals based on hybrid feature selection and transfer learning, *Expert Systems with Applications* 137 (2019) 266–280.
- [5] Y. Cui, Y. Xu, D. Wu, EEG-Based Driver Drowsiness Estimation Using Feature Weighted Episodic Training, *IEEE Trans. on Neural Systems and Rehabilitation Engineering* 27 (11) (2019) 2263–2273.
- [6] M. Dai, D. Zheng, S. Liu, P. Zhang, Transfer kernel common spatial patterns for motor imagery brain-computer interface classification, *Computational and Mathematical Methods in Medicine* 2018.
- [7] A. Delorme, S. Makeig, EEGLAB: an open source toolbox for analysis of single-trial EEG dynamics including independent component analysis, *Journal of Neuroscience Methods* 134 (2004) 9–21.
- [8] P. T. Fletcher, S. Joshi, Principal geodesic analysis on symmetric spaces: Statistics of diffusion tensors, *Lecture Notes in Computer Science* 3117 (2004) 87–98.
- [9] H. He, D. Wu, Different Set Domain Adaptation for Brain-Computer Interfaces: A Label Alignment Approach, *IEEE Trans. on Neural Systems and Rehabilitation Engineering* 28 (5) (2020) 1091–1108.
- [10] H. He, D. Wu, Transfer Learning for Brain-Computer Interfaces: A Euclidean Space Data Alignment Approach, *IEEE Trans. on Biomedical Engineering* 67 (2) (2020) 399–410.
- [11] V. Jayaram, M. Alamgir, Y. Altun, B. Scholkopf, M. Grosse-Wentrup, Transfer learning in brain-computer interfaces, *IEEE Computational Intelligence Magazine* 11 (1) (2016) 20–31.
- [12] I. Jolliffe, *Principal Component Analysis*, Wiley Online Library, 2002.
- [13] I. Kononenko, Estimating attributes: Analysis and extensions of RELIEF, in: Proc. European Conf. on Machine Learning, Catania, Italy, 171–182, 1994.

- [14] D. Kostas, F. Rudzicz, Thinker invariance: enabling deep neural networks for BCI across more people, *Journal of Neural Engineering* 17 (5) (2020) 056008.
- [15] T. D. Lagerlund, F. W. Sharbrough, N. E. Busacker, Spatial Filtering of Multichannel Electroencephalographic Recordings Through Principal Component Analysis by Singular Value Decomposition, *Journal of Clinical Neurophysiology* 14 (1) (1997) 73–82.
- [16] B. J. Lance, S. E. Kerick, A. J. Ries, K. S. Oie, K. McDowell, Brain-Computer Interface Technologies in the Coming Decades, *Proc. of the IEEE* 100 (3) (2012) 1585–1599.
- [17] V. J. Lawhern, A. J. Solon, N. R. Waytowich, S. M. Gordon, C. P. Hung, B. J. Lance, EEGNet: a compact convolutional neural network for EEG-based brain-computer interfaces, *Journal of Neural Engineering* 15 (5) (2018) 056013.
- [18] C.-T. Lin, C. Chuang, Y. Hung, C. Fang, D. Wu, Y.-K. Wang, A Driving Performance Forecasting System Based on Brain Dynamic State Analysis Using 4-D Convolutional Neural Networks, *IEEE Trans. on Cybernetics* In press.
- [19] S. R. Liyanage, C. Guan, H. Zhang, K. K. Ang, J. Xu, T. H. Lee, Dynamically weighted ensemble classification for non-stationary EEG processing, *Journal of Neural Engineering* 10 (3) (2013) 036007.
- [20] M. Long, J. Wang, G. Ding, S. J. Pan, P. S. Yu, Adaptation Regularization: A General Framework for Transfer Learning, *IEEE Trans. on Knowledge and Data Engineering* 26 (5) (2014) 1076–1089.
- [21] M. Long, J. Wang, J. Sun, S. Y. Philip, Domain invariant transfer kernel learning, *IEEE Trans. on Knowledge and Data Engineering* 27 (6) (2015) 1519–1532.
- [22] F. Lotte, Signal Processing Approaches to Minimize or Suppress Calibration Time in Oscillatory Activity-Based Brain-Computer Interfaces, *Proc. of the IEEE* 103 (6) (2015) 871–890.
- [23] F. Lotte, L. Bougrain, A. Cichocki, M. Clerc, M. Congedo, A. Rakotomamonjy, F. Yger, A review of classification algorithms for EEG-based brain-computer interfaces: a 10 year update, *Journal of Neural Engineering* 15 (3) (2018) 031005.
- [24] H. Lu, H.-L. Eng, C. Guan, K. N. Plataniotis, A. N. Venetsanopoulos, Regularized common spatial pattern with aggregation for EEG classification in small-sample setting, *IEEE Trans. on Biomedical Engineering* 57 (12) (2010) 2936–2946.
- [25] A. Marathe, V. Lawhern, D. Wu, D. Slayback, B. Lance, Improved neural signal classification in a rapid serial visual presentation task using active learning, *IEEE Trans. on Neural Systems and Rehabilitation Engineering* 24 (3) (2016) 333–343.
- [26] M. Moakher, A differential geometric approach to the geometric mean of symmetric Positive-Definite matrices, *SIAM Journal on Matrix Analysis and Applications* 26 (3) (2005) 735–747.

- [27] L. F. Nicolas-Alonso, J. Gomez-Gil, Brain computer interfaces, a review, *Sensors* 12 (2) (2012) 1211–1279.
- [28] S. J. Pan, Q. Yang, A survey on transfer learning, *IEEE Trans. on Knowledge and Data Engineering* 22 (10) (2010) 1345–1359.
- [29] H. Peng, F. Long, C. Ding, Feature selection based on mutual information criteria of max-dependency, max-relevance, and min-redundancy, *IEEE Trans. on Pattern Analysis and Machine Intelligence* 27 (8) (2005) 1226–1238.
- [30] X. Pennec, P. Fillard, N. Ayache, A Riemannian framework for tensor computing, *International Journal of Computer Vision* 66 (1) (2006) 41–66.
- [31] G. Pfurtscheller, G. R. Müller-Putz, R. Scherer, C. Neuper, Rehabilitation with brain-computer interface systems, *Computer* 41 (10) (2008) 58–65.
- [32] G. Pfurtscheller, C. Neuper, Motor imagery and direct brain-computer communication, *Proc. of the IEEE* 89 (7) (2001) 1123–1134.
- [33] H. Ramoser, J. Muller-Gerking, G. Pfurtscheller, Optimal spatial filtering of single trial EEG during imagined hand movement, *IEEE Trans. on Rehabilitation Engineering* 8 (4) (2000) 441–446.
- [34] R. P. Rao, R. Scherer, Chapter 10 - Statistical Pattern Recognition and Machine Learning in Brain-Computer Interfaces, in: K. G. Oweiss (Ed.), *Statistical Signal Processing for Neuroscience and Neurotechnology*, Academic Press, Oxford, 335–367, 2010.
- [35] B. Rivet, A. Souloumiac, V. Attina, G. Gibert, xDAWN algorithm to enhance evoked potentials: application to brain-computer interface, *IEEE Trans. on Biomedical Engineering* 56 (8) (2009) 2035–2043.
- [36] P. L. C. Rodrigues, C. Jutten, M. Congedo, Riemannian Procrustes Analysis: Transfer Learning for Brain-Computer Interfaces, *IEEE Trans. on Biomedical Engineering* 66 (8) (2019) 2390–2401.
- [37] R. N. Roy, S. Bonnet, S. Charbonnier, P. Jallon, A. Campagne, A comparison of ERP spatial filtering methods for optimal mental workload estimation, in: *Proc. 37th Annual Int’l Conf. of the IEEE Engineering in Medicine and Biology Society (EMBC)*, 7254–7257, 2015.
- [38] S. Saha, K. I. U. Ahmed, R. Mostafa, L. Hadjileontiadis, A. Khandoker, Evidence of Variabilities in EEG Dynamics During Motor Imagery-Based Multiclass Brain-Computer Interface, *IEEE Trans. on Neural Systems and Rehabilitation Engineering* 26 (2) (2018) 371–382.
- [39] R. T. Schirrmeister, J. T. Springenberg, L. D. J. Fiederer, M. Glasstetter, K. Eggensperger, M. Tangermann, F. Hutter, W. Burgard, T. Ball, Deep learning with convolutional neural networks for EEG decoding and visualization, *Human Brain Mapping* 38 (11) (2017) 5391–5420.

- [40] M. Teplan, Fundamentals of EEG measurement, *Measurement Science Review* 2 (2) (2002) 1–11.
- [41] J. van Erp, F. Lotte, M. Tangermann, Brain-Computer Interfaces: Beyond Medical Applications, *Computer* 45 (4) (2012) 26–34, ISSN 0018-9162.
- [42] P. Wang, J. Lu, B. Zhang, Z. Tang, A Review on Transfer Learning for Brain-Computer Interface Classification, in: *Proc. 5th Int’l Conf. on Information Science and Technology*, Changsha, China, 2015.
- [43] J. R. Wolpaw, N. Birbaumer, D. J. McFarland, G. Pfurtscheller, T. M. Vaughan, Brain-computer interfaces for communication and control, *Clinical Neurophysiology* 113 (6) (2002) 767–791.
- [44] D. Wu, Online and Offline Domain Adaptation for Reducing BCI Calibration Effort, *IEEE Trans. on Human-Machine Systems* 47 (4) (2017) 550–563.
- [45] D. Wu, J.-T. King, C.-H. Chuang, C.-T. Lin, T.-P. Jung, Spatial Filtering for EEG-Based Regression Problems in Brain-Computer Interface (BCI), *IEEE Trans. on Fuzzy Systems* 26 (2) (2018) 771–781.
- [46] D. Wu, B. J. Lance, V. J. Lawhern, Transfer Learning and Active Transfer Learning for Reducing Calibration Data in Single-Trial Classification of Visually-Evoked Potentials, in: *Proc. IEEE Int’l Conf. on Systems, Man, and Cybernetics*, San Diego, CA, 2014.
- [47] D. Wu, V. J. Lawhern, S. Gordon, B. J. Lance, C.-T. Lin, Driver Drowsiness Estimation from EEG Signals Using Online Weighted Adaptation Regularization for Regression (OwARR), *IEEE Trans. on Fuzzy Systems* 25 (6) (2017) 1522–1535.
- [48] D. Wu, V. J. Lawhern, W. D. Hairston, B. J. Lance, Switching EEG headsets made easy: Reducing offline calibration effort using active weighted adaptation regularization, *IEEE Trans. on Neural Systems and Rehabilitation Engineering* 24 (11) (2016) 1125–1137.
- [49] D. Wu, V. J. Lawhern, B. J. Lance, S. Gordon, T.-P. Jung, C.-T. Lin, EEG-Based User Reaction Time Estimation Using Riemannian Geometry Features, *IEEE Trans. on Neural Systems and Rehabilitation Engineering* 25 (11) (2017) 2157–2168.
- [50] D. Wu, Y. Xu, B.-L. Lu, Transfer Learning for EEG-Based Brain-Computer Interfaces: A Review of Progress Made Since 2016, *IEEE Trans. on Cognitive and Developmental Systems* In press.
- [51] L. Xu, M. Xu, Y. Ke, X. An, S. Liu, D. Ming, Cross-dataset Variability Problem in EEG Decoding with Deep Learning, *Frontiers in Human Neuroscience* 14 (2020) 103.

- [52] F. Yger, M. Berar, F. Lotte, Riemannian approaches in brain-computer interfaces: a review, *IEEE Trans. on Neural Systems and Rehabilitation Engineering* 25 (10) (2017) 1753–1762.
- [53] P. Zanini, M. Congedo, C. Jutten, S. Said, Y. Berthoumieu, Transfer Learning: a Riemannian geometry framework with applications to Brain-Computer Interfaces, *IEEE Trans. on Biomedical Engineering* 65 (5) (2018) 1107–1116.
- [54] W. Zhang, D. Wu, Manifold Embedded Knowledge Transfer for Brain-Computer Interfaces, *IEEE Trans. on Neural Systems and Rehabilitation Engineering* 28 (5) (2020) 1117–1127.